


Screening of Diagnostic Biomarkers and Immune Infiltration Characteristics Linking Rheumatoid Arthritis and Rosacea Based on Bioinformatics Analysis

Yun Wang¹, Jun Chen¹, Zheng-Yu Shen¹, Jie Zhang², Yu-Jie Zhu¹, Xu-Qiong Xia¹ 

¹Department of Dermatology, Shanghai Ninth People's Hospital Affiliated Shanghai JiaoTong University School of Medicine, Shanghai, 200080, People's Republic of China; ²The International Peace Maternity and Child Health Hospital, School of Medicine, Shanghai Jiao Tong University, Shanghai, People's Republic of China

Correspondence: Yu-Jie Zhu; Xu-Qiong Xia, Email zhuyujie@sh9hospital.org.cn; xiaxuqiong@outlook.com

Introduction: Both rheumatoid arthritis (RA) and rosacea represent common chronic systemic autoimmune conditions. Recent research indicates a heightened RA risk among individuals with rosacea. However, the molecular mechanisms linking these diseases remain largely unknown. This study aims to uncover shared molecular regulatory networks and immune cell infiltration patterns in both rosacea and RA.

Methods: The gene expression profiles of RA (GSE12021, GSE55457), and the rosacea gene expression profile (GSE6591), were downloaded from Gene Expression Omnibus (GEO) databases, and obtained to screen differentially expressed genes (DEGs) by using “limma” package in R software. Various analyses including GO, KEGG, protein–protein interaction (PPI) network, and weighted gene co-expression network analyses (WGCNA) were conducted to explore potential biological functions and signaling pathways. CIBERSORT was used to assess the abundance of immune cells. Pearson coefficients were used to calculate the correlations between overlapped genes and the leukocyte gene signature matrix. Flow cytometry (FCM) analysis confirmed the most abundant immune cells detected in rheumatoid arthritis and rosacea. Receiver operator characteristic (ROC) analysis, enzyme-linked immunosorbent assay (ELISA), and qRT-PCR were used to confirm biomarkers and functions.

Results: Two hundred seventy-seven co-expressed DEGs were identified from these datasets. Functional enrichment analysis indicated that these DEGs were associated with immune processes and chemokine-mediated signaling pathways. Fourteen and 17 hub genes overlapped between cytoHubba and WGCNA were identified in RA and rosacea, respectively. Macrophages and dendritic cells were RA and rosacea's most abundant immune cells, respectively. The ROC curves demonstrated potential diagnostic values of CXCL10 and CCL27, showing higher levels in the serum of patients with RA or rosacea, and suggesting possible regulation in the densities and functions of macrophages and dendritic cells from RA and rosacea, which were validated by FCM and qRT-PCR.

Conclusion: Importantly, our findings may contribute to the scientific basis for biomarkers and therapeutic targets for patients with RA and rosacea in the future.

Keywords: autoimmune disease, immune infiltration, macrophage, chemokine, diagnostic biomarkers

Introduction

One of the most common chronic systemic autoimmune diseases is called rheumatoid arthritis (RA), primarily affecting the joints,^{1–3} with an incidence ranging from 0.5% to 2%.¹ RA predominantly affects middle-aged women aged 40–60 years.^{1,4} Chronic synovitis of affected joint is the main clinical manifestation of RA, which characterized as pannus formation, persistent synovitis, and synovial hyperplasia.⁵ Human leukocyte antigen (HLA) system is known to have a significant influence on the pathogenesis of RA.¹ Additionally, cytokines and chemokines also play an essential role by activating endothelial cells and recruiting immune cells to accumulate within the synovial compartment, leading to bony

erosions.^{6,7} Immune cells have a substantial impact on the onset and progression of RA, highlighting the need for further research to comprehend the immune mechanisms of RA in the synovium.¹ Therefore, identifying key genes and evaluating the influence of immune cells is essential.

Another chronic systemic inflammatory condition known as rosacea, categorized as a type of dermatological disorder,⁸ affects both genders equally.⁹ The incidence of it is 1 to 22 per 100 people.¹⁰ Clinical features include persistent facial redness, small solid elevations, pus-filled lesions, widened blood vessels, and repeated sudden reddening.^{11–13} The etiology involves dysregulation of the body's immune responses, vascular and neuronal abnormalities, genetic factors, and microorganisms like demodex folliculorum.¹¹ Genetic studies have indicated common risk loci between rosacea and autoimmune conditions like type 1 diabetes mellitus (T1DM), and RA.^{14,15} Moreover, more and more studies have shown an increased risk of RA in individuals with rosacea.^{16,17} Given the significant involvement of immune cells in the pathogenesis of these diseases, understanding the profile of inflammatory cell infiltration between RA and rosacea could provide insights into their immunopathogenesis and identify new therapeutic targets.

Active transcriptomic and microarray analyses are extensively utilized in various autoimmune diseases to discover new biomarkers and enhance the diagnosis and treatment.¹⁸ The integration of microarray and bioinformatics analyses facilitates the investigation of potential pivotal genes and pathway networks that closely relate to disease progression.

In this study, we utilized bioinformatics analysis to uncover essential biological functions, regulatory networks of transcriptional factor (TF), key targets, and infiltration of immune cell in pathological processes of RA and rosacea. This research aims to enhance our comprehension of inflammatory occurrences that culminate in RA and rosacea, as well as potential therapeutic strategies directed at immune cells.

Materials and Methods

Differentially Expressed Genes in RA and Rosacea

As shown in [Figure 1](#), two independent RA gene expression profiles (GSE12021, and GSE55457) were downloaded from Gene Expression Omnibus (GEO) database (<https://www.ncbi.nlm.nih.gov/geo/>): 21 synovial membrane samples from 9 normal controls, and 12 RA patients in GSE12021 (GPL96 platform), and 23 synovial membrane samples from 10 normal controls, and 13 RA patients in GSE55457 (GPL96 platform). The 38 rosacea tissues and 20 control tissues in GSE65914 (GPL570 platform) were also downloaded from GEO. In order to remove batch effect, we used the “sva” R package (version 4.2.3; <https://www.r-project.org/>), which identified and built surrogate variables for high-dimensional data sets. What was used for background correction and quantile normalization of all the raw data files is the “limma” package¹⁹ in R software (version 4.2.3; <https://www.r-project.org/>). And then, we got the expression values. The averages of the probe set of values were calculated as the expression values for the same gene with multiple probe sets.²⁰ The “limma” package was utilized to identify the differentially expressed genes (DEGs) between control and disease samples.¹⁹ Furthermore, a volcano plot was created to evaluate the DEGs. Genes with $|\log_2$ fold change (FC) ≥ 1 and an adjusted P value of < 0.05 were considered as differentially expressed between disease and control tissues.

Identification of Co-Expressed Genes

After retrieving RA and rosacea DEGs separately, the DEGs were utilized to obtain the intersection of RA DEGs and rosacea DEGs using R software, as mentioned in previous studies.²¹ These concurrently dysregulated DEGs in both RA and rosacea could play a key role in connecting the two conditions, and we refer to them as co-expressed genes.

Functional Enrichment of DEGs

The Gene Ontology (GO) analysis, and Kyoto Encyclopedia of Genes and Genomes (KEGG) pathway analysis of co-expressed genes were carried out by using R software and the “clusterProfiler” package.²² In this analysis, symbol codes were first converted to Entrez ID using Human genome annotation package “org.Hs.eg.db”, and the “ggplot2”,²³ “pathview”²⁴ and “gplots” packages of R software²⁵ were used to visualize the plots.

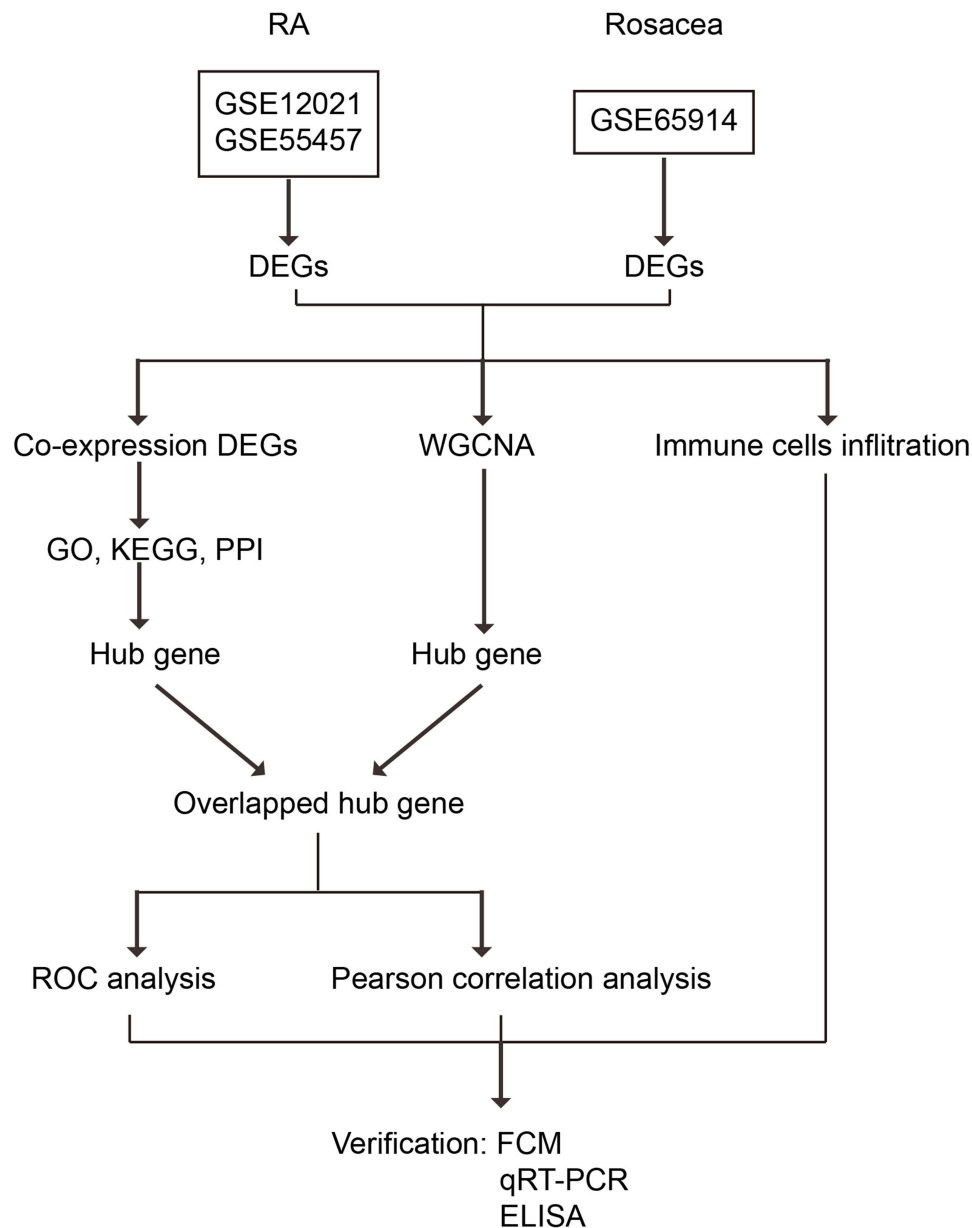


Figure 1 Study flowchart.

Abbreviations: GSE, gene expression omnibus series; WGCNA, weighted gene co-expression network analysis; DEGs, differentially expressed genes; GO, gene ontology; KEGG, Kyoto encyclopedia of genes and genomes; FCM, flow cytometry analysis; ELISA, enzyme-linked immunosorbent assay; and qRT-PCR, quantitative real-time polymerase chain reaction.

Protein–Protein Interaction (PPI) Network Analysis

The STRING database (available online: <http://string-db.org>) was performed for PPI network prediction. Cytoscape (v. 3.8.1) was used for visual representation and further PPI network experimental studies. “cytoHubba” is a plug-in unit for calculating the weight of each gene and exploring the hub genes of the PPI network, and “MCODE” is a plug-in unit for identifying the representative modules using Cytoscape software.^{26,27}

Weighted Gene Co-Expression Network Analysis (WGCNA) and Module Gene Selection

The system biology approach of Weighted Gene Co-expression Network Analysis (WGCNA) was utilized to investigate the gene correlations. The “WGCNA” package²⁸ in R version 4.2.3 was employed for the analysis. Firstly, the median

absolute deviation (MAD) of each gene was calculated, and 50% of genes with the smallest MAD were removed. Secondly, the differential gene expression matrix was filtered using the `goodSamplesGenes` function to eliminate unqualified genes and samples, and a scale-free co-expression network was constructed. Thirdly, the adjacency was computed using the “soft” thresholding power (β) derived from co-expression similarity, which was then transformed into a topological overlap matrix (TOM), thereby determining gene ratio and dissimilarity. Fourthly, modules were detected through hierarchical clustering and a dynamic tree cut function. Genes with identical expression profiles were classified into modules using average linkage hierarchical clustering, with a TOM-based dissimilarity metric and a minimum gene group size of 30 for the gene dendrogram. Fifthly, the dissimilarity of module eigengenes was computed, a cut line was selected for the module dendrogram, and several modules were combined for further investigation. The eigengene network was then visualized. WGCNA analysis was applied to identify essential modules in rheumatoid arthritis (RA) and rosacea.

Identification of Overlapped Hub Genes

After identifying hub genes by using Cytoscape software or WGCNA of RA and rosacea separately, they were imported into R software to obtain the intersection of them. These jointly dysregulated genes may be the keys to the links between the two, and we call them overlapped hub genes.

Immune Infiltration Analysis

The normalized gene expression profiles of RA, and rosacea were used for identifying different immune cell types of tissues, which was analyzed by CIBERSORT.²⁹ Which contains 547 genes for distinguishing 22 human hematopoietic cell phenotypes, is called LM22, a kind of leukocyte gene signature matrix. CIBERSORT results matched ground truth phenotypes in 93% of external datasets of variably purified leukocyte subsets.²⁹ Based on the analysis of LM22, a matrix of 22 kinds of immune cells was obtained. CIBERSORT $P < 0.05$ was used to filter the samples, and the percentage of each immune cell type in the samples was calculated and displayed in a bar plot. The “box” package was used to compare the levels of 22 kinds of immune cells between the two groups. The “ggplot2” package²³ was adopted to visualize the plots.

Correlation of Overlapped Genes with 22 Kinds of Immune Cells

We investigated the role of overlapped genes in regulating the connection between RA and rosacea by obtaining the expression profiles of overlapped genes and 22 types of leukocyte gene signature matrix, and analyzing correlations using Pearson coefficients. The `Hmisc` package (version 4.4.1) was utilized to calculate Pearson correlation coefficient (r) values and screen genes with moderate and strong correlation (P -values < 0.05 and $|r| > 0.4$).³⁰ Additionally, a heatmap of the correlation between overlapped genes and 22 types of leukocyte gene signature matrix was generated using the `corrplot` package (version 0.84).

ROC Analysis

The receiver operator characteristic (ROC) curves were plotted and area under curve (AUC) was calculated separately to evaluate the performance of each model using the R packages “pROC”. And $AUC > 0.7$ indicated that the model had a good fitting effect.

Patients' Recruitment for the Cohort of Validation

The protocol for this study was approved by the Human Research Ethics Committees of Shanghai Ninth People's Hospital Affiliated Shanghai JiaoTong University School of Medicine, and written informed consent was obtained from all participants. Whole blood was collected from patients attending the dermatology department and rheumatology department and diagnosed as rosacea and RA. Rosacea is characterized by recurrent episodes of flushing, persistent erythema, inflammatory papules/pustules, and telangiectasia.³¹ The diagnostic criteria of rosacea are based on the guidelines published by the National Rosacea Society Expert Committee.¹² The diagnosis of RA is based on the 2010 American College of Rheumatology (ACR)/European League Against Rheumatism (EULAR) classification criteria.³²

Application of these criteria provides a score of 0–10, with a score of ≥ 6 being satisfactory for the diagnosis of definite RA. Blood samples of patients with rosacea or RA were used to test the concentration of CXCL10/CCL27 by enzyme-linked immunosorbent assay (ELISA). The blood samples from healthy control were used to isolate PBMCs by Ficoll-Hypaque (Sigma-Aldrich, 26,873–85-8) density gradient centrifugation at 800 g for 30 min and prepared for the following research. PBMCs were collected to isolate macrophages or DC cells by MASC (Miltenyi Biotec, 130–050-201, or 130–100-777) for in vitro experiments.

Elisa

According to the method provided by the manufacturer (Invitrogen, KAC2361; Invitrogen, KAC2361), CXCL10/CCL27 concentration in the serum of patients with rheumatoid arthritis and rosacea is measured using monoclonal antibodies against CXCL10/CCL27 that are coated onto a plate. The serum sample is incubated for a period of time, followed by the addition of biotinylated secondary antibodies. The absorbance is determined at a wavelength of 450nm, and CXCL10/CCL27 concentration in the sample is calculated.

Cells

Macrophages were treated with recombinant human (rHs) CXCL10 (MedChemExpress, HY-P700533) (0 ng/mL, 2 ng/mL) for 24 h. DC cells were treated with recombinant human (rHs) CCL27 (MedChemExpress, HY-P7767) (0 ng/mL, 2 ng/mL) for 24 h. Both of macrophages and DC cells were collected and used to isolated RNA to detect relative genes expressions by using quantitative real-time polymerase chain reaction (qRT-PCR).

Quantitative Real-Time Polymerase Chain Reaction (qRT-PCR)

The RNA extraction was carried out using TRIzol reagent (Invitrogen, Carlsbad, CA, USA), as previously described.²¹ Subsequently, the concentration and purity of the RNA were quantified using a NanoDrop spectrophotometer (NanoDrop Technologies; Thermo Fisher Scientific, MA, USA). The PrimeScript RT Reagent Kit (TaKaRa Biotechnology, Co., Ltd., Dalian, China) was employed to perform reverse transcription of the total RNA to cDNA. Next, qRT-qPCR was conducted with SYBR Green PCR Master Mix (TaKaRa Biotechnology). The qRT-PCR primers can be found in Table 1. The target mRNA expressions were normalized to ACTB expression. All reactions were processed using the Applied Biosystems 7500 Real-Time PCR System (Thermo Fisher Scientific, MA, USA). The test results were analyzed using the $2^{-\Delta\Delta C_t}$ method.

Flow Cytometry Analysis (FCM)

Flow cytometry analysis (FCM) was used to validate the main changes in immunocytes. All antibodies were from Biotend (San Diego, CA, USA). The antibodies to detect dendritic cells (DC) and macrophages included: APC/Cyanine 7 (APC/Cy7)-conjugated anti-human CD45, fluorescein isothiocyanate (FITC)-conjugated anti-human CD86, brilliant violet (BV) 605-conjugated anti-human CD206, PE-Cy7-conjugated anti-human CD14, PE-conjugated

Table 1 Primer Sequences of Each Gene Detected in RT-PCR

Gene		Sequence
ACTB	Forward	5'-GCCGACAGGATGCAGAAGGAGATCA-3'
	Reverse	5'-AAGCATTGCGGTGGACGATGGA-3'
IL-1 β	Forward	ATGATGGCTTATTACAGTGGCAA
	Reverse	GTCGGAGATTCGTAGCTGGA
IL-6	Forward	ACTCACCTCTTCAGAACGAATTG
	Reverse	CCATCTTTGGAAGGTTTCAGGTTG
IFN- α	Forward	TCGGTAACTGACTTGAATGTCCA
	Reverse	TCGCTTCCCTGTTTTAGCTGC
TNF- α	Forward	GAGGCCAAGCCCTGGTATG
	Reverse	CGGGCCGATTGATCTCAGC

anti-human CXCL10, BV 510-conjugated anti-human HLA-DR, FITC-conjugated anti-human CD1a, and Biotin conjugated anti-human CCL27. Flow cytometry protocol for Anti-CCL27 antibody was the manufacturer's protocols (ab186421, Abcam, UK). After being treated with the aforementioned antibodies, the cells underwent two washes and were then suspended in PBS for FCM analysis. The samples were examined using a CytoFLEX flow cytometer (Beckman Coulter, Inc), and the data were analyzed utilizing FlowJo (version 10.07, FlowJo LLC), as detailed in a previous study.²¹

Statistical Analysis

Statistical analysis utilized SPSS (version 23.0, Chicago, IL) or R software. Mean \pm standard deviation (SD) was employed to represent continuous variables, and differences between the two groups were assessed using Student's *t*-test for normally distributed variables. The comparison of continuous variables with a non-normal distribution was conducted using a Kruskal–Wallis *H*-test with Dunn's multiple-comparisons test, and the results were conveyed as the median and interquartile range. Statistically significant differences were identified when $P < 0.05$.

Results

Identification and Enrichment Analysis of DEGs

There was a total of 4304 DEGs identified in the RA combined dataset by using the “limma” method, of which 1961 were upregulated and 2343 were downregulated. [Figure 2A](#) and [B](#) display the heatmap and volcano plot of RA DEGs. For the rosacea dataset, 1024 DEGs were identified (636 upregulated and 388 downregulated), as shown in [Figure 2C](#) and [D](#).

The Co-Expressed DEGs and Enriched Pathways in Both RA and Rosacea

A total of 277 common differentially expressed genes (DEGs) have been identified in both rheumatoid arthritis (RA) and rosacea ([Figure 3A](#)). These genes play a role in immune processes and chemokine-mediated signaling pathways, as revealed by GO enrichment analysis ([Figure 3B](#)). Additionally, KEGG enrichment analysis has shown their connection to chemokine pathways and antigen binding ([Figure 3C](#)). Consistent with these findings, data from the Metascape database have indicated enrichment of inflammation, chemokine, and cytokine-related pathways ([Figure 3D](#)). Furthermore, enrichment analysis by DisGeNET, a comprehensive discovery platform for genes and variants associated with human diseases,³³ has underscored their relevance to skin, autoimmunity, inflammation, and infection-related diseases ([Figure 3E](#)). The analysis of transcription factor–target interactions in the TRRUST database suggested that many of these common DEGs are regulated by transcription factors, indicating a potential key role of the transcription factor regulatory network in the progression of RA and rosacea ([Figure 3F](#)).

PPI Network, and Identification of Hub Genes

The important modules were identified following the performance of the PPI enrichment analysis ([Figure 4A](#)). The three MCODE components isolated were predominantly linked to the cytokine signaling pathway, interferon signaling, and TCR signaling ([Figure 4B](#)). To further assess the significance of the genes in the PPI network of DEGs, the top 10 hub genes were obtained from the PPI network by using cytoHubba in 5 patterns and illustrated in [Figure 4C](#). The occurrence of these hub genes was computed and presented in [Figure 4D](#), suggesting that CXCL10, CCR7, SAA1, CCR5 may play crucial roles.

WGCNA and Key Module Identification

In this research, we employed WGCNA to pinpoint the most correlated module in RA and rosacea. A total of 30 modules were identified in the RA databases, and 8 modules in the rosacea dataset, with each color representing a different module. A heatmap was then generated to depict module-trait relationships based on the Spearman correlation coefficient to assess the association between each module and the respective disease ([Figure 5A–F](#)). The turquoise module, which comprised 605 genes, exhibited the highest correlation with RA (correlation coefficient = 0.79, $p = 7.9 * 10^{-9}$) and was considered the pivotal module for subsequent analysis. Furthermore, the correlations between module membership and

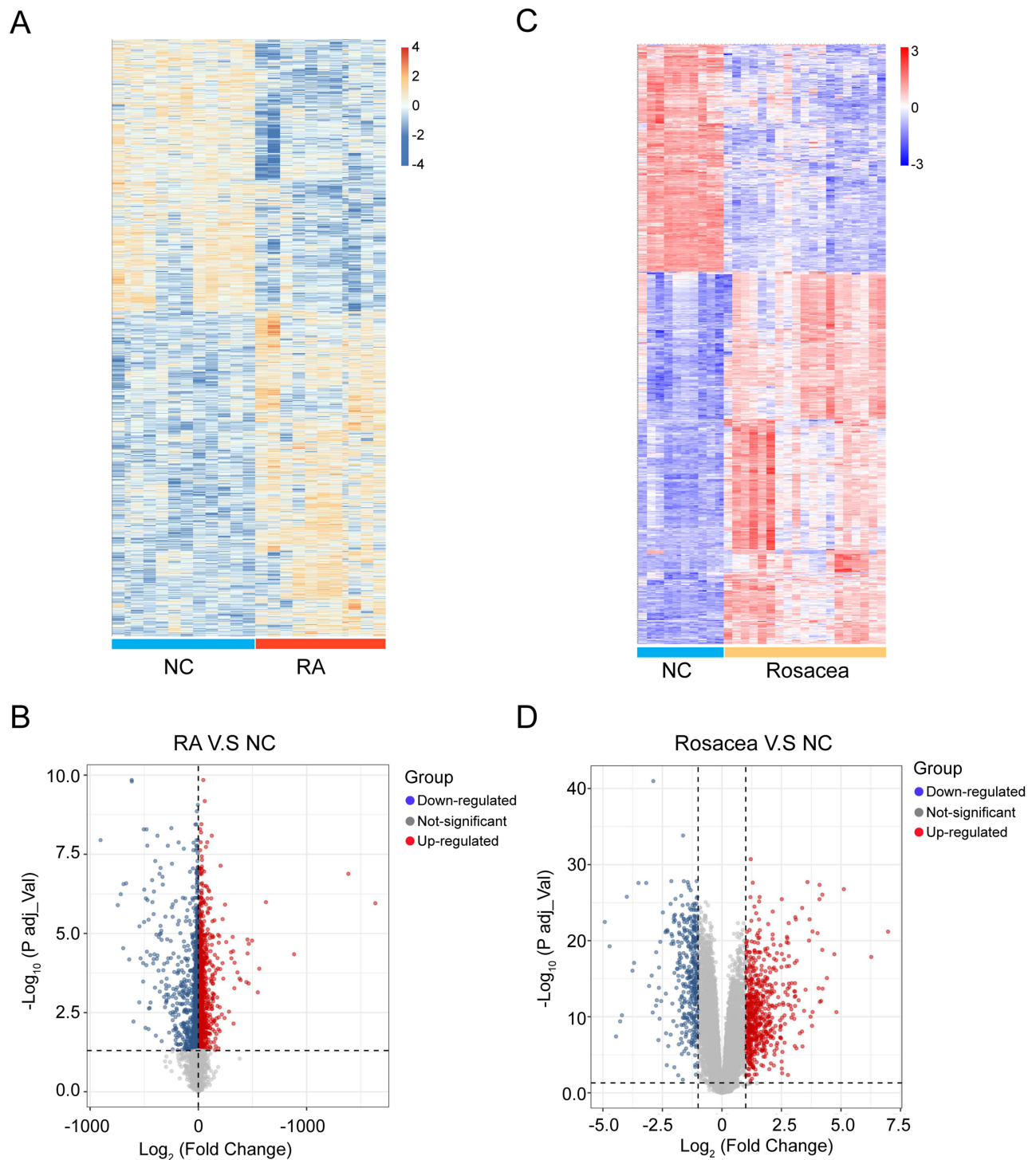


Figure 2 Heatmap and volcano plot for the DEGs identified from the RA and rosacea datasets. **(A)** DEGs were showed in rows, and the samples of RA cases or controls were showed in columns. The Orange and blue represent DEGs with upregulated and downregulated gene expression, respectively. **(B)** Red, blue and gray plot dots represent DEGs in RA cases or control with upregulated, downregulated gene and not-significant expression, respectively. **(C)** DEGs were showed in rows, and the samples of rosacea cases or controls were showed in columns. The red and blue represent DEGs with upregulated and downregulated gene expression, respectively. **(D)** Red, blue and gray plot dots represent DEGs in rosacea cases or control with upregulated, downregulated gene and not-significant expression, respectively. NC, normal controls.

gene significance in the turquoise module for RA were calculated, revealing a significant positive correlation ($r = 0.79$) as depicted in [Figure 5C](#). Similarly, in the case of rosacea, the pink module, holding 541 genes, demonstrated the highest correlation with rosacea (correlation coefficient = 0.80, $p = 2.54 \times 10^{-12}$) and was considered the pivotal module for

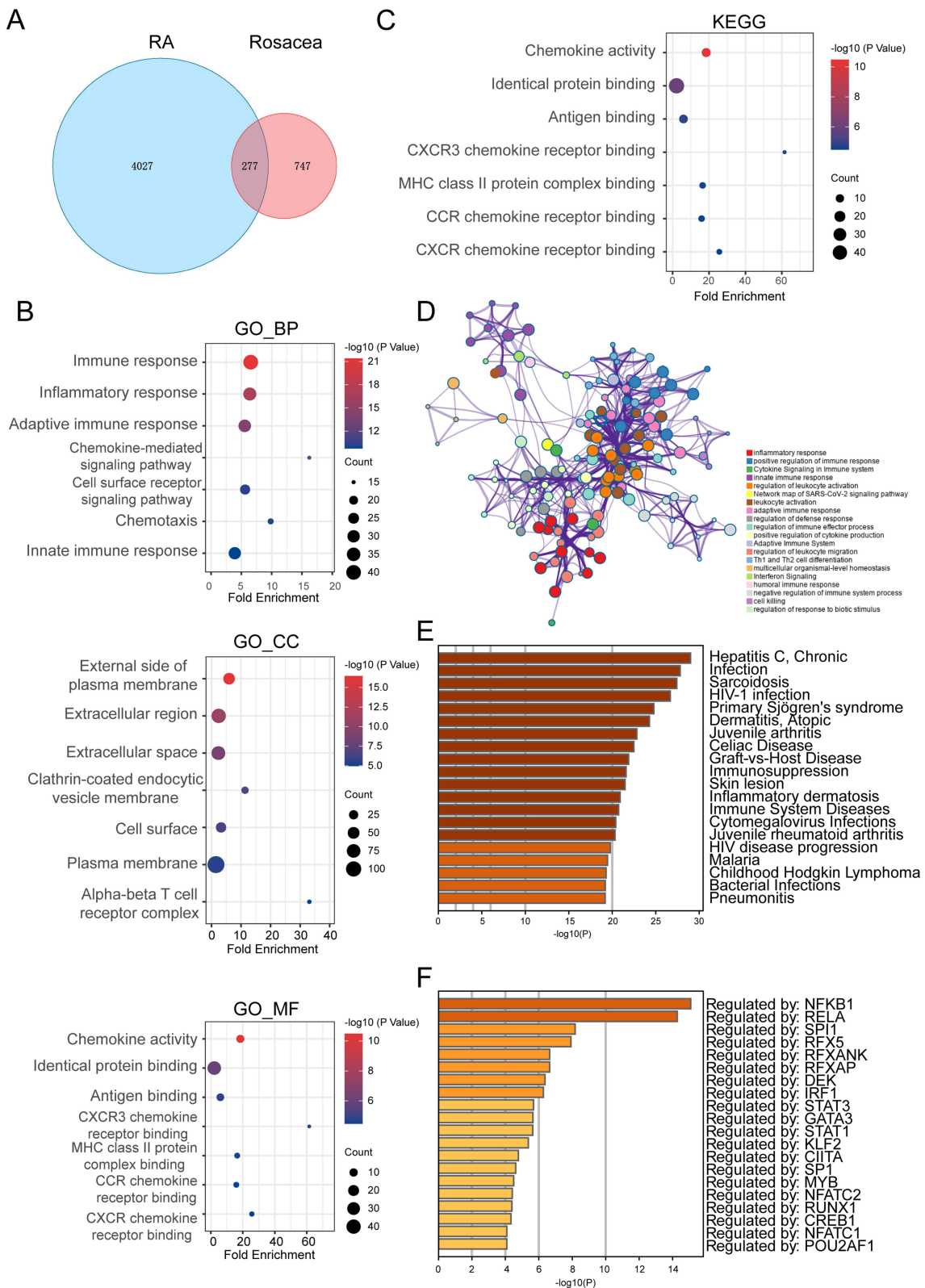


Figure 3 The Co-Expressed DEGs and Enriched Pathways in Both RA and Rosacea. **(A)** The Venn graph of co-expressed DEGs in both RA and rosacea. **(B)** GO enrichment analysis of co-expressed DEGs. **(C)** The KEGG analysis of co-expressed DEGs. **(D)** The pathway enrichment analysis of co-expressed DEGs using Metascape (<http://metascape.org/gp/index>). **(E)** The disease enrichment analysis of co-expressed DEGs in DisGeNET using Metascape (<http://metascape.org/gp/index>). **(F)** The transcription factor (TF) enrichment analysis of co-expressed DEGs in TRRUST using Metascape (<http://metascape.org/gp/index>).

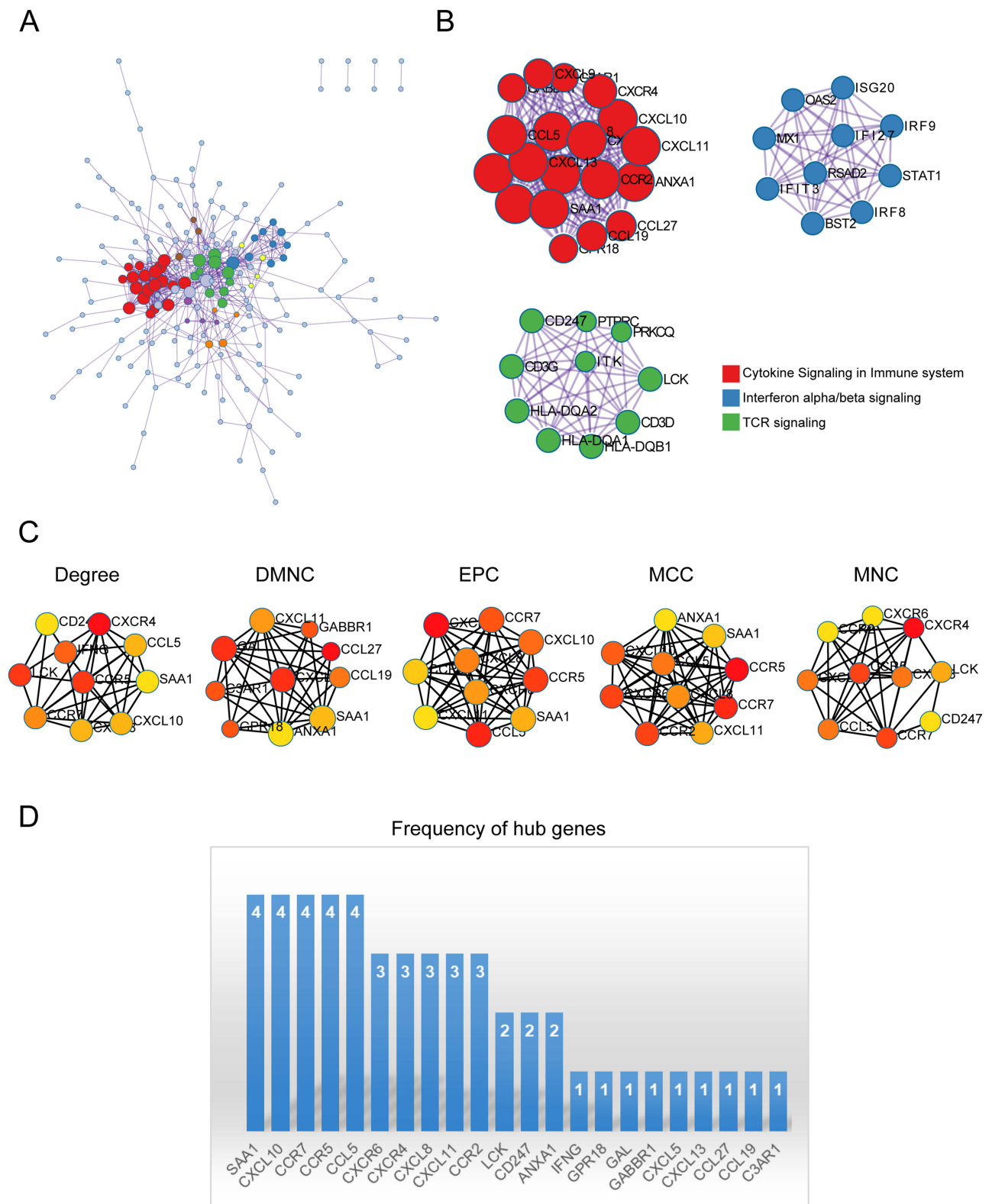


Figure 4 PPI network, and Identification of Hub Genes. **(A)** PPI network constructed with the co-expressed DEGs in both RA and rosacea. **(B)** MCODE was used to identify the significant module from the PPI network with a score of ≥ 5.0 . Different nodes' color present different functions. **(C)** The top 10 hub genes of 5 patterns were discovered by Cytoscape software (version 3.7.2, cytoHubba plug-ins). **(D)** The frequency of hub genes.

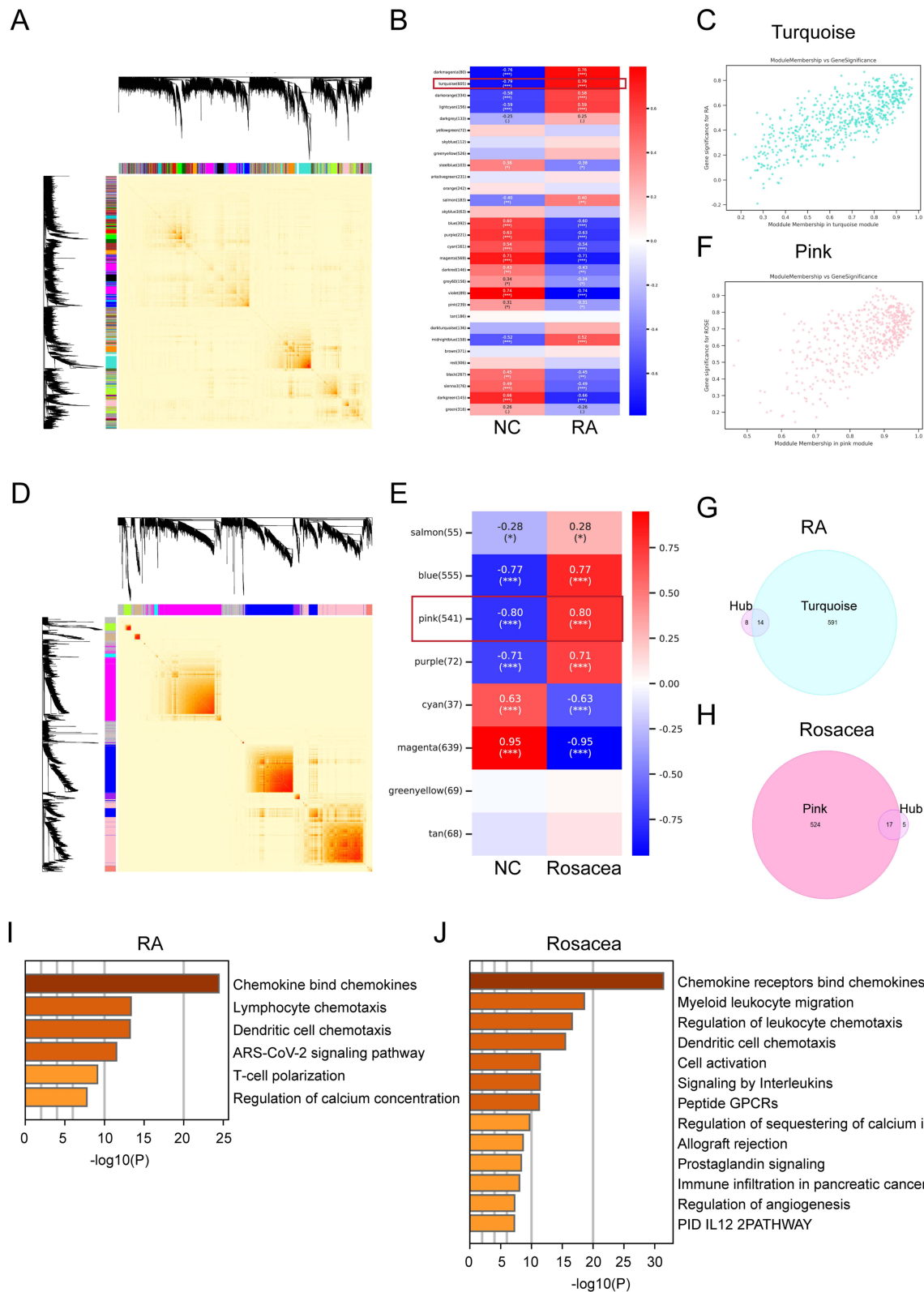


Figure 5 Identification of key module genes via WGCNA in RA and rosacea. **(A)** Gene co-expression modules represented by different colors under the gene tree in RA. **(B)** Module–trait relationships in RA. Each cell contains the corresponding correlation and p-value. **(C)** The correlation between RA and key module genes. **(D)** Gene co-expression modules represented by different colors under the gene tree in rosacea. **(E)** Module–trait relationships in rosacea. Each cell contains the corresponding correlation and p-value. **(F)** The correlation between rosacea and key module genes. **(G)** The Venn graph of overlapped DEGs in both hub gene got from Figure 4C and key module genes got from WGCNA in RA. **(H)** The Venn graph of overlapped DEGs in both hub gene got from Figure 4C and key module genes got from WGCNA in rosacea. *, $p < 0.05$; ***, $p < 0.001$. **(I)** The pathway enrichment analysis of overlapped hub DEGs in RA using Metascape (<http://metascape.org/gp/index>). **(J)** The pathway enrichment analysis of overlapped hub DEGs in rosacea using Metascape (<http://metascape.org/gp/index>). NC, normal controls.

subsequent analysis. The correlations between module membership and gene significance in the pink module for rosacea were also calculated, showing a significant positive correlation ($r = 0.80$) as shown in Figure 5F. To further investigate the essential genes in RA and rosacea, hub genes obtained from cytoHubba (Figure 4C) and WGCNA were used, leading to the identification of 14 and 17 overlapping hub genes in RA and rosacea, respectively (Figure 5G and H). Furthermore, we examined the enrichment of various pathways was analyzed in overlapping hub genes, such as chemokine signaling, lymphocyte/DC chemotaxis, and immune infiltration, in both RA and rosacea (Figure 5I and J).

The Patterns of Immune Cell Infiltration in RA and Rosacea

What was particularly significant was the functional enrichment analysis of DEGs exhibited a significant enrichment of immune response in both RA and rosacea. Furthermore, we conducted the CIBERSORT algorithm to compare the abundance of 22 types of immune cells in RA and rosacea databases (Figure 6). The percentage of each immune cell type in every sample from RA databases is depicted in the bar plot (Figure 6A), showing that M2 macrophages predominated in RA tissues (Figure 6B). The boxplot illustrating the levels of immune cell infiltration was ordered based on their median proportion in the RA group, suggesting that M2 macrophages were the most abundant immune cells, with their proportion reduced in RA patients (Figure 6C). The bar plot as shown in Figure 6D is the proportions of each immune cell type in every sample from rosacea databases. DC cells were more prevalent in rosacea patients (Figure 6E). In rosacea patients, the boxplot illustrating the levels of immune cell infiltration was ordered based on their median proportion suggesting that the number of DC cells was lower compared to the normal control (NC) group (Figure 6F).

The Correlation Between Infiltrated Immune Cells and Overlapped Hub Genes

In order to explore the correlation between infiltrated immune cells and overlapped hub genes, correlations were analyzed by calculating Pearson coefficients. As the data shown in Figure 7A and B, M1 macrophages, the data from RA databases showed that $CD8^+$ T cells, T cells gamma delta, and other three kinds of cells were positively associated with overlapped hub genes. M2 macrophages, T cells CD4 memory resting, and another 10 types of cells were negatively correlated with overlapped hub genes. As the data shown in Figure 7C and D, the data from rosacea databases showed that M0 macrophages, T cells CD4 memory active, T cells gamma delta, and other three kinds of cells were positively associated with overlapped hub genes. DC cells, mast cells resting, and another 7 types of cells were negatively correlated with overlapped hub genes. The RA gene expression profiles result showed that the expression level of CXCL10 was increased in patients with RA, which was positively correlated with M1 macrophages ($R = 0.87$, $p = 2.49 \times 10^{-12}$) (Figure 7E and F). The rosacea gene expression profiles result showed that the expression level of CCL27 was decreased in patients with rosacea, which was positively correlated with DC resting ($R = 0.54$, $p = 1.07 \times 10^{-5}$) (Figure 7G and H). These findings indicate that CXCL10 and CCL27 could impact the stimulation and activity of immune cells in patients with RA and rosacea.

The Validation of Infiltrated Immune Cells and Diagnostic Biomarkers

The results of the ROC analysis suggested that CXCL10 and CCL27 might serve as potential diagnostic biomarkers for rheumatoid arthritis and rosacea, respectively (Figure 8A and B). Furthermore, ELISA results showed that the serum CXCL10 concentration significantly increases in patients of RA, and the serum CCL27 concentration from patients with rosacea was higher than that in normal controls (Figure 8A and B). The proportion of macrophages was elevated in RA group, along with the abnormal M1 and M2 macrophages ratio, measured by FCM analysis (Figure 8C and D). The number of DC cells was found to be declined in rosacea patients (Figure 8E and F). Additionally, the in vitro CXCL10-induced macrophage stimulation can elevate the transcription of the inflammatory cytokines in macrophages (Figure 8G). Furthermore, CCL27 can promote the expression of a higher number of inflammatory genes in DC cells (Figure 8H). These results suggest that CXCL10 and CCL27 play a crucial role in the homing of immune cells in RA and rosacea. However, further experimentation is necessary to validate these findings. These molecules hold promise as significant biomarkers for future clinical detection of RA or rosacea.

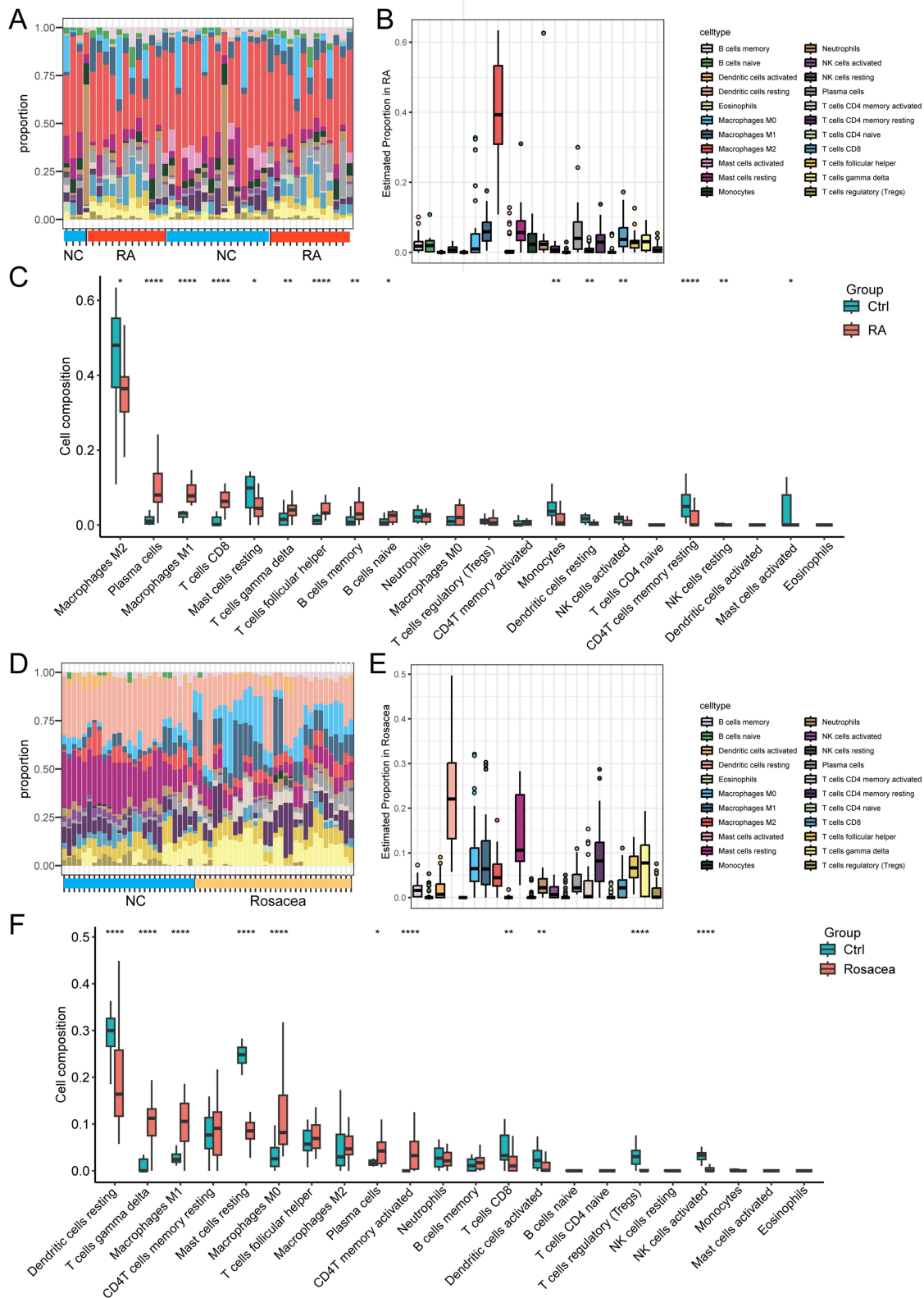


Figure 6 The infiltration pattern of immune cells among different groups. **(A)** The relative percentage of 22 types of immune cells in RA datasets, and each column refers to one of the samples of RA cases or controls. **(B)** The relative percentage of 22 types of immune cells in all samples of RA databases. **(C)** The difference of immune infiltration between RA and controls. The control group was marked as blue color and RA group was marked as red color. **(D)** The relative percentage of 22 types of immune cells in RA datasets, and each column refers to one of the samples of rosacea cases or controls. **(E)** The relative percentage of 22 types of immune cells in all samples of rosacea databases. **(F)** The difference of immune infiltration between rosacea and controls. The control group was marked as blue color and rosacea group was marked as red color. *, p < 0.05; **, p < 0.01; ***, p < 0.001, ****, p < 0.0001. NC, normal controls.

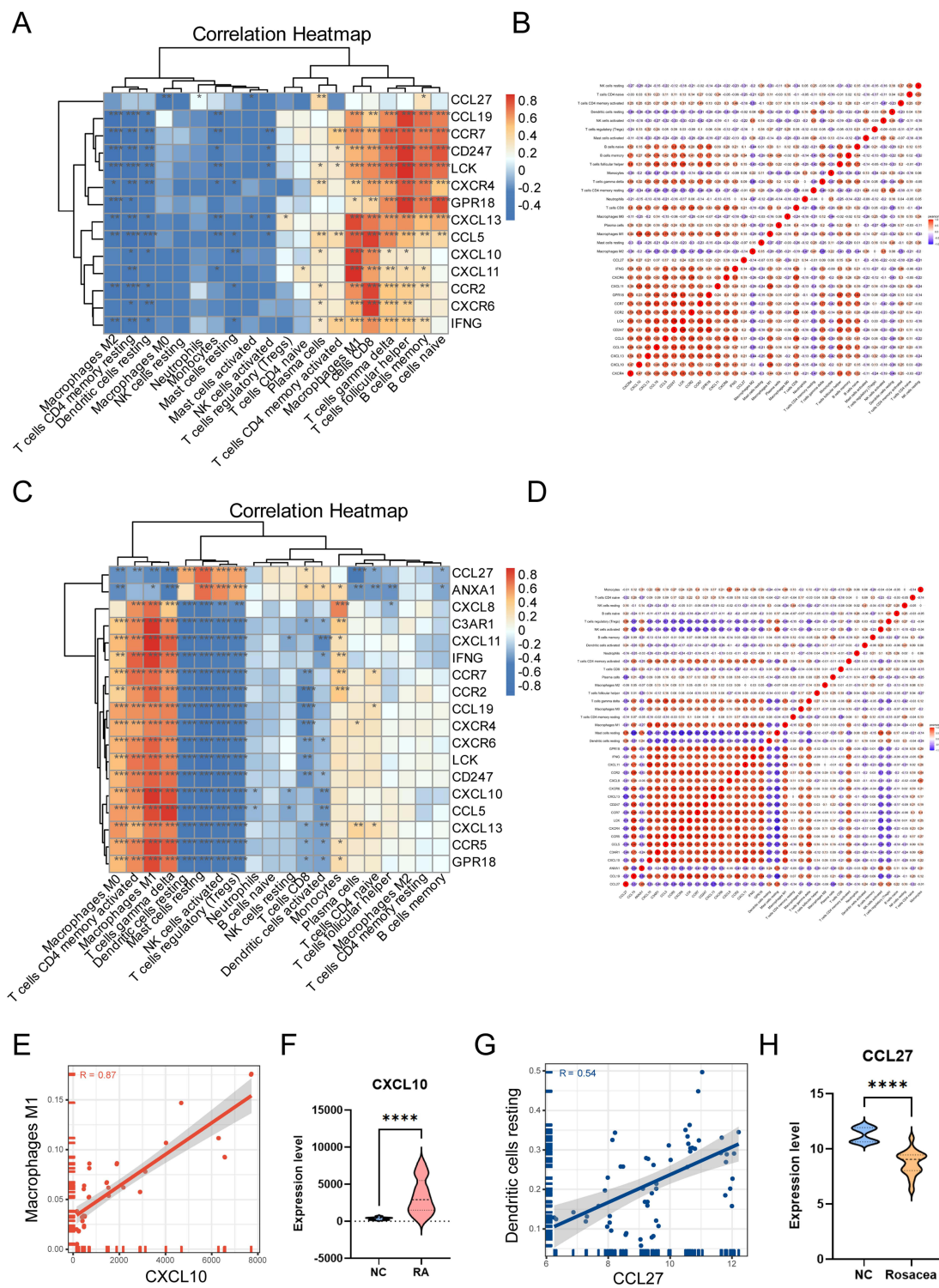


Figure 7 The correlation between infiltrated immune cells and overlapped hub genes. **(A)** The heatmap showed the correlation between infiltrated immune cells and overlapped hub genes in RA. The darker the color, the stronger the correlation. Blue graph represents negative correlation, whereas red graph represents positive correlation between infiltrated immune cells and overlapped hub genes. **(B)** The bubble plot showed correlation coefficients (**R**) among each kind of infiltrated immune cells and every single overlapped hub gene in RA. **(C)** The heatmap showed the correlation between infiltrated immune cells and overlapped hub genes in rosacea. The darker the color, the stronger the correlation. Blue graph represents negative correlation, whereas red graph represents positive correlation between infiltrated immune cells and overlapped hub genes. **(D)** The bubble plot showed correlation coefficients (**R**) among each kind of infiltrated immune cells and every single overlapped hub gene in rosacea. **(E)** The correlation between CXCL10 and M1 macrophages in RA. **(F)** The expression level of CXCL10 in RA and control. **(G)** The correlation between CCL27 and dendritic cells resting in rosacea. **(H)** The expression level of CCL27 in rosacea and control. Data are presented as the mean \pm standard error of the mean. Statistical significance (Student's *t*-test): *, $p < 0.05$; **, $p < 0.01$; ***, $p < 0.001$. NC, normal controls.

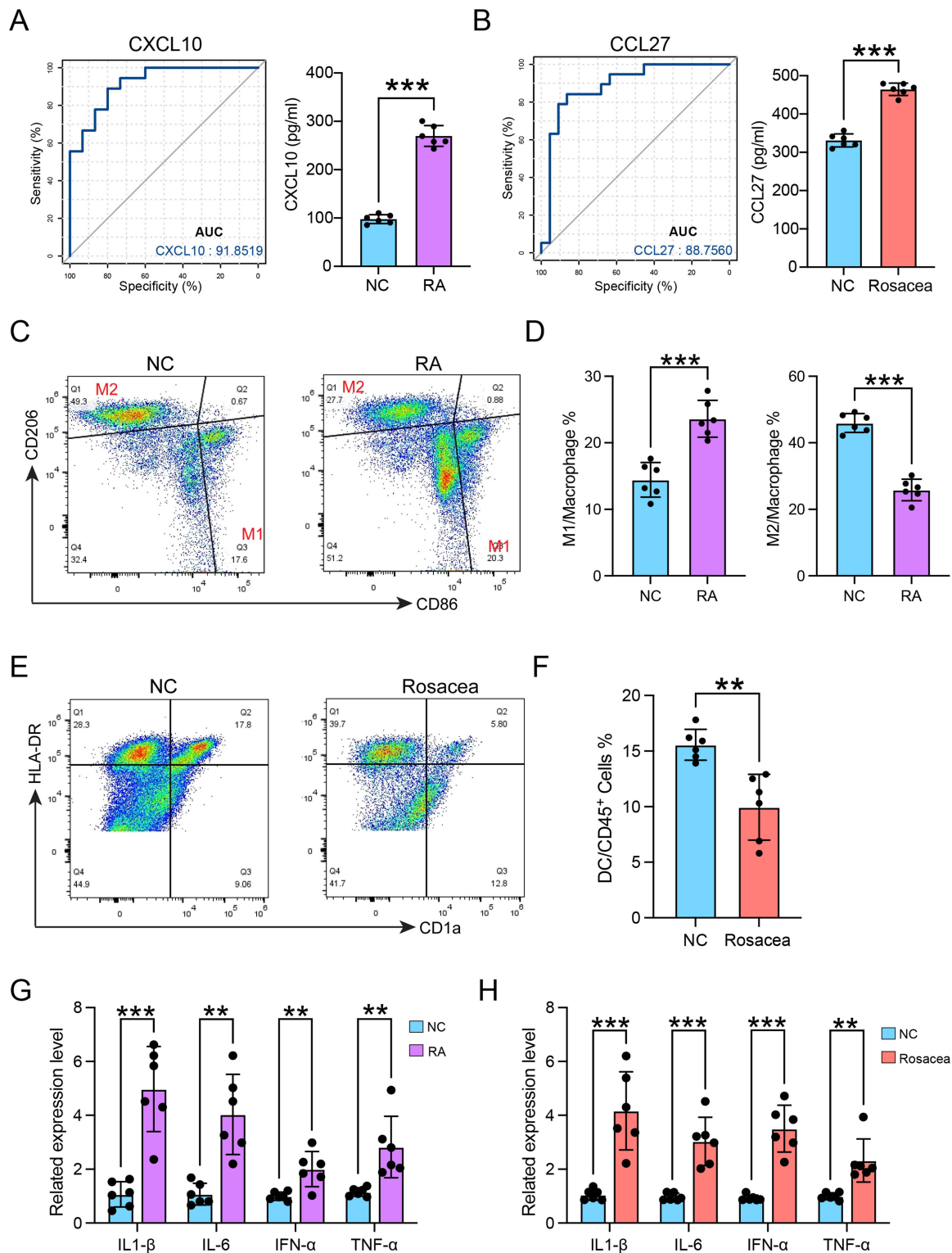


Figure 8 The validation of infiltrated immune cells and diagnostic biomarkers. **(A)** The diagnostic effectiveness of CXCL10 for RA by ROC analysis (left), and the serum CXCL10 concentration in patients of RA (right). **(B)** The diagnostic effectiveness of CCL27 for RA by ROC analysis (left), and the serum CCL27 concentration in patients of rosacea (right). **(C)** The gating strategy for identifying M1 macrophages and M2 macrophages from CD45⁺ cells. **(D)** The quantitative analysis of the proportions of M1 and M2 macrophages in control and patients with RA (n=6). **(E)** The gating strategy for identifying DC cells from CD45⁺ cells. **(F)** The quantitative analysis of the proportions of DC cells in control and patients (n=6) with rosacea. **(G)** The mRNA expression levels of TNF- α , IL-6, IL-1 β , and IFN- α in macrophages separated from patients with RA or normal control (NC) after CXCL10 treatment for 24h. **(H)** The mRNA expression levels of TNF- α , IL-6, IL-1 β , and IFN- α in DC cells separated from patients with rosacea or normal control (NC) after CCL27 treatment for 24h. Data are presented as the mean \pm standard error of the mean. Statistical significance (Student's *t*-test): ***p* < 0.01, ****p* < 0.001. NC, normal controls.

Discussion

Similar to RA, rosacea is a common type of chronic inflammatory diseases. Innate and adaptive immune responses play a crucial role in the development of both RA and rosacea.^{34,35} However, the precise relationship between RA and rosacea is still not fully understood. This research identified common genes with differentially expressed between RA and rosacea, created an immune cell atlas, and discovered diagnostic biomarkers of RA and rosacea.

An increasing body of research indicates that the crucial factor in the development of synovitis and persistent joint damage involves the intricate interaction and activation of infiltrating immune cells.^{1,36} Indeed, the dysregulation of vasculature and immunology is crucial to the pathogenesis of rosacea.³⁷ This study identified 277 co-expressed DEGs, which were significantly enriched in immune-, and chemokine-related pathways. Furthermore, the enrichment analysis revealed that these co-expressed DEGs were linked to diseases such as infection-, immunosuppression-, skin lesion-, and juvenile rheumatoid arthritis (JRA) according to DisGeNET. These findings suggest that inflammatory- and chemokine-related pathways play a vital role in the pathogenesis of RA and rosacea.

The infiltration of 22 different types of immune cells was examined in RA and rosacea using the CIBERSORT method. This method analyzes 22 subsets of immune cells in complex tissues based on normalized bulk transcriptome profiles.²⁹ In RA synovial tissues, compared to the normal control, there was a significant increase in plasma cells, M1 macrophages, CD8⁺T cells, $\gamma\delta$ T cells, helper T cells, and memory B cells, positively correlated with common hub genes. While M2 macrophages, resting mast cells, and monocytes showed a significant decrease, consistent with other studies, and showed a negative correlation with common hub genes.³⁶ The study observed an abnormal polarization of macrophages into M1/M2 phenotypes in RA, which was supported by previous research.^{38,39} Macrophages secrete a variety of pro-inflammatory cytokines, chemokines, angiogenic factors, and degrading enzymes, contributing significantly to tissue damage.⁴⁰ Macrophages in RA patients' serum showed decreased levels of TNF- α , IL-6, IL-1 β , and IL-23, various CXCL and CCL chemokines, which play a role in recruiting and activating polymorphonuclear cells (PMNs), T cells, B cells, and monocytes thereby promoting and sustaining inflammation.⁴¹ Furthermore, macrophages contribute to the increased vascularity in RA by producing angiogenic factors, such as vascular endothelial growth factor (VEGF), transforming growth factor (TGF) α/β or TNF α .⁴² Additionally, macrophages regulate the expressions of Receptor Activator of Nuclear Factor Kappa-B Ligand (RANKL) and matrix metalloproteinases (MMPs), which are implicated in articular surface erosions.⁴⁰ The elevated immune cell levels in RA patients are positively correlated with overlapped hub genes. Previous studies have highlighted the involvement of CXCL10 and its receptor CXCR3 in the pathogenesis of various autoimmune diseases.⁴² In our current research, we observed an up-regulation of CXCL10 expression in RA patients, which was positively associated with M1 macrophages. High levels of CXCL10 serve as a marker for the host immune response, particularly in RA synovium, where it is primarily produced by infiltrating macrophage-like cells and fibroblast-like synoviocytes.⁴³

In rosacea patients, higher proportions of M1 macrophages, $\gamma\delta$ T cells, M0 macrophages, plasma cells, memory activated CD4⁺T cells were observed, positively correlated with common hub genes. Conversely, lower proportions of resting DC cells, resting mast cells, CD8⁺T cells, and regulatory T cells (Treg) showed a negative correlation with common hub genes. According to the data, the infiltration M1 macrophages in rosacea tissues increased, and can be activated through pattern recognition receptors (PPRs) or TLRs 2 and 4 on Langerhans cells (LC).⁴⁴ This activation leads to an increase in the induction of inflammatory cytokines, especially IL-10 and TNF- α .⁴⁵ The resting DC cells in skin tissue known as Langerhans cells (LC), were significantly lower in rosacea samples compared to normal controls, which is in line with previous study.⁴⁵ Heat-shock proteins (HSPs) binding to the TLRs expressed on LC may trigger the apoptotic pathway or induce their migration to regional lymph nodes, resulting in a reduction in the epidermal LC density.^{45,46} TNF- α , IL-6, IL-1 β , and IFN- α were observed to decrease in serum of patients with rosacea in this study. This decrease was linked to induced reactive oxygen species (ROS) production and an active MAPK-NF- κ B signal in keratinocyte cells, promoting inflammatory responses, and angiogenesis in rosacea.⁴⁷ Additionally, a positive correlation was found between the density of resting DC cells and CCL27, which was down-regulated in rosacea. CCL27, also known as T-cell attracting chemokine (CTACK), has been implicated in various tumor-related pathological processes, such as tumor progression, metastasis and immune escape.⁴⁶ The interaction between CCL27 and its receptor CCR10

plays a role in recruiting Tregs.^{48,49} In rosacea lesions, reduced CCL27 expression causes a decrease in Treg cells. Our study demonstrated that with CCL27 treatment resulted in DC cells expressing higher level of proinflammatory factors. This outcome underscores the intricate interplay between immune cells influencing rosacea pathogenesis, pointing towards the need for further investigations to validate this potential mechanism.

Base on the co-expressed DEGs, we uncovered the TF regulatory network in RA/rosacea, with NF- κ B, and RelA identified as the top 2 TFs influencing the pathogenesis of RA and rosacea. In various human disease processes, especially inflammatory conditions and cancer, NF- κ B signaling plays a crucial role.³⁷ In RA, NF- κ B and RANKL contribute to inflammatory response and bone erosion.⁵⁰ CXCL10 has been recognized as a key cytokine that leads to increased RANKL expression in RA synovial tissue,⁵¹ which is also elevated in the serum of patients with RA.⁵¹ In rosacea, stimulation of Toll-like receptors (TLRs) results in an accumulation of active NF- κ B, and LL-37, an anti-microbial protein cathelicidin.⁵² These factors promote angiogenesis, stimulate leukocyte chemotaxis, and are involved in the production of proinflammatory cytokines.³⁶ Additionally, post-translational modification of RelA, particularly phosphorylation, are responsible for the abnormal activation of NF- κ B.⁵³

After identifying the overlapped hub genes through the analysis of Protein-Protein Interaction (PPI) network and Weighted Gene Co-expression Network Analysis (WGCNA), it was observed that a majority of these genes were chemokines, including CXCL10, CCR7, CCR5, CCL27. The core genes were found to be associated with functions related to chemokine signaling, lymphocyte/DC cells chemotaxis, T cell polarization, among others. The interaction between chemokine receptors and cytokines leads to the recruitment of immune cells to abnormal clusters in the synovial membrane or skin surface, consequently advancing the disease progression, through the secretion of abundant cytokines, chemokines, and degrading enzymes.^{54,55} The physiological roles of chemokines in tumor, including activities like proliferation, drug resistance, migration, invasion, and organ-specific metastasis of tumor cells, as well as the effects on angiogenesis and lymphangiogenesis, have been extensively investigated.⁵⁶ Several monoclonal antibodies targeting chemokines have been utilized in cancer treatment therapy. Moreover, CCL27 has been identified as a reliable marker for predicting the response to Bacillus Calmette-Guerin (BCG) therapy in non-muscle-invasive bladder cancer (NMIBC).⁵⁷ CXCL10 has been recognized as a crucial target in patients with metastatic non-small cell lung cancer (mNSCLC) undergoing pemetrexed and cisplatin (PEM/CDDP) chemotherapy.⁵⁸ Notably, in the context of RA and rosacea pathogenesis, CXCL10 and CCL27 have emerged as pivotal elements. These findings indicated that CXCL10 and CCL27 could potentially serve as biomarkers of RA and rosacea, respectively.

This study encountered specific limitations. First and foremost, rheumatoid arthritis (RA) and rosacea, as inflammatory conditions, not only demonstrate abnormal immune cell infiltration in the affected area, but also present an imbalanced immune cell microenvironment in the peripheral blood. Therefore, a comprehensive analysis of gene expression profiles of peripheral blood mononuclear cells for these two conditions is essential to pinpoint additional crucial co-pathogenic genes. Secondly, our analysis solely focused on the variations in the two primary groups of immune cells in RA and rosacea, indicating a necessity for further investigation to ascertain if other cell subtypes also contribute to the onset and progression of the diseases. Lastly, additional experiments are imperative to validate that CXCL10 and CCL27 serve as biomarkers for the clinical diagnosis of RA and rosacea, respectively.

Conclusion

Our research indicates that RA and rosacea have common genetic markers, providing potential for innovative molecular marker screening in clinical practice. Moreover, both conditions display comparable immune cell infiltration conditions display comparable immune cell M1 macrophages. Our results suggest that CXCL10 and CCL27 could serve as biomarkers for RA and rosacea, presenting a promising therapeutic avenue for future treatments of patients with these conditions.

Data Sharing Statement

Publicly available datasets were analyzed in this study. This data can be found here: <https://www.ncbi.nlm.nih.gov/geo/>; GSE11021, GSE55457, and GSE65914. The code associated with the current study is available in the [github] repository, <https://github.com/doctorxia203/FII-2023>.

Ethics Approval and Consent to Participate

The protocol for this study was approved by the Human Research Ethics Committees of Shanghai Ninth People's Hospital Affiliated Shanghai JiaoTong University School of Medicine (NO. SH9H-2022-T265-1), was in keeping with the principles of the Declaration of Helsinki and written informed consent was obtained from all participants.

Acknowledgments

The authors would like to pay tribute to the patients and investigators who participated in the GEO and provided data selflessly.

Author Contributions

All authors made a significant contribution to the work reported, whether that is in the conception, study design, execution, acquisition of data, analysis and interpretation, or in all these areas; took part in drafting, revising or critically reviewing the article; gave final approval of the version to be published; have agreed on the journal to which the article has been submitted; and agree to be accountable for all aspects of the work.

Funding

This study was supported by National Natural Science Foundation of China (62273231), Original Exploration Project of Shanghai Ninth People's Hospital, Shanghai Jiaotong University School of Medicine (JYYC005), and Interdisciplinary Program of Shanghai Jiao Tong University (YG2022QN063).

Disclosure

The authors declare that they have no competing interests in this work.

References

1. Smolen JS, Aletaha D, McInnes IB. Rheumatoid arthritis. *Lancet*. 2016;388(10055):2023–2038. doi:10.1016/S0140-6736(16)30173-8
2. Gibofsky A. Epidemiology, pathophysiology, and diagnosis of rheumatoid arthritis: A Synopsis. *Am J Manag Care*. 2014;20(7):S128–135.
3. Orr C, Vieira-Sousa E, Boyle DL, et al. Synovial tissue research: a state-of-The-art review. *Nat Rev Rheumatol*. 2017;13(10):630. doi:10.1038/nrrheum.2017.161
4. Aletaha D, Smolen JS. Diagnosis and management of rheumatoid arthritis: A review. *JAMA*. 2018;320(13):1360–1372. doi:10.1001/jama.2018.13103
5. McInnes IB, Schett G. Pathogenetic insights from the treatment of rheumatoid arthritis. *Lancet*. 2017;389(10086):2328–2337. doi:10.1016/S0140-6736(17)31472-1
6. Pettit AR, Ji H, von Stechow D, et al. TRANCE/RANKL knockout mice are protected from bone erosion in a serum transfer model of arthritis. *Am J Pathol*. 2001;159(5):1689–1699. doi:10.1016/S0002-9440(10)63016-7
7. Redlich K, Hayer S, Ricci R, et al. Osteoclasts are essential for TNF-alpha-mediated joint destruction. *J Clin Invest*. 2002;110(10):1419–1427. doi:10.1172/JCI0215582
8. van Zuuren EJ, Fedorowicz Z. Interventions for Rosacea. *JAMA*. 2015;314(22):2403–2404. doi:10.1001/jama.2015.15287
9. Gether L, Overgaard LK, Egeberg A, Thyssen JP. Incidence and prevalence of rosacea: a systematic review and meta-analysis. *Br J Dermatol*. 2018;179(2):282–289. doi:10.1111/bjd.16481
10. Tan J, Berg M. Rosacea: current state of epidemiology. *J Am Acad Dermatol*. 2013;69(6):S27–35. doi:10.1016/j.jaad.2013.04.043
11. van Zuuren EJ, Solomon CG. Rosacea. *N Engl J Med*. 2017;377(18):1754–1764. doi:10.1056/NEJMc1506630
12. Thiboutot D, Anderson R, Cook-Bolden F, et al. Standard management options for rosacea: The 2019 update by the national rosacea society expert committee. *J Am Acad Dermatol*. 2020;82(6):1501–1510. doi:10.1016/j.jaad.2020.01.077
13. Gallo RL, Granstein RD, Kang S, et al. Standard classification and pathophysiology of rosacea: The 2017 update by the national rosacea society expert committee. *J Am Acad Dermatol*. 2018;78(1):148–155. doi:10.1016/j.jaad.2017.08.037
14. Efferth T, Oesch F. The immunosuppressive activity of artemisinin-type drugs towards inflammatory and autoimmune diseases. *Med Res Rev*. 2021;41(6):3023–3061. doi:10.1002/med.21842
15. Torfs CP, King MC, Huey B, Malmgren J, Grumet FC. Genetic interrelationship between insulin-dependent diabetes mellitus, the autoimmune thyroid diseases, and rheumatoid arthritis. *Am J Hum Genet*. 1986;38(2):170–187.
16. Chae K, Cho M, Kim S, Woo YR. Increased risk of rheumatoid arthritis in patients with rosacea: a nationwide population-based cohort study. *J Eur Acad Dermatol Venereol*. 2023;37(11):e1336–e1338. doi:10.1111/jdv.19316
17. Haber R, El Gemayel M. comorbidities in rosacea: a systematic review and update. *J Am Acad Dermatol*. 2018;78(4):786–792e788. doi:10.1016/j.jaad.2017.09.016
18. Li WC, Bai L, Xu Y, et al. Identification of differentially expressed genes in synovial tissue of rheumatoid arthritis and osteoarthritis in patients. *J Cell Biochem*. 2019;120(3):4533–4544. doi:10.1002/jcb.27741

19. Ritchie ME, Phipson B, Wu D, et al. limma powers differential expression analyses for RNA-sequencing and microarray studies. *Nucleic Acids Res.* 2015;43(7):e47. doi:10.1093/nar/gkv007
20. Li W, Li K, Zhao L, Zou H. Bioinformatics analysis reveals disturbance mechanism of MAPK signaling pathway and cell cycle in Glioblastoma multiforme. *Gene.* 2014;547(2):346–350. doi:10.1016/j.gene.2014.06.042
21. Lai ZZ, Zhang J, Zhou WJ, et al. Identification of potential biomarkers and immune infiltration characteristics in recurrent implantation failure using bioinformatics analysis. *Front Immunol.* 2023;14:992765. doi:10.3389/fimmu.2023.992765
22. Yu G, Wang LG, Han Y, He QY. clusterProfiler: an R package for comparing biological themes among gene clusters. *OMICS.* 2012;16(5):284–287. doi:10.1089/omi.2011.0118
23. Walter W, Sanchez-Cabo F, Ricote M. GOplot: an R package for visually combining expression data with functional analysis. *Bioinformatics.* 2015;31(17):2912–2914. doi:10.1093/bioinformatics/btv300
24. Luo W, Brouwer C. Pathview: an R/Bioconductor package for pathway-based data integration and visualization. *Bioinformatics.* 2013;29(14):1830–1831. doi:10.1093/bioinformatics/btt285
25. Wickham H. *ggplot2: Elegant Graphics for Data Analysis.* New York: Springer-Verlag New York; 2016.
26. Bader GD, Hogue CW. An automated method for finding molecular complexes in large protein interaction networks. *BMC Bioinf.* 2003;4:2. doi:10.1186/1471-2105-4-2
27. Shannon P, Markiel A, Ozier O, et al. Cytoscape: a software environment for integrated models of biomolecular interaction networks. *Genome Res.* 2003;13(11):2498–2504. doi:10.1101/gr.1239303
28. Langfelder P, Horvath S. WGCNA: an R package for weighted correlation network analysis. *BMC Bioinf.* 2008;9:559. doi:10.1186/1471-2105-9-559
29. Newman AM, Liu CL, Green MR, et al. Robust enumeration of cell subsets from tissue expression profiles. *Nat Methods.* 2015;12(5):453–457. doi:10.1038/nmeth.3337
30. Akoglu H. User's guide to correlation coefficients. *Turk J Emerg Med.* 2018;18(3):91–93. doi:10.1016/j.tjem.2018.08.001
31. van Zuuren EJ, Arents BWM, van der Linden MMD, Vermeulen S, Fedorowicz Z, Tan J. Rosacea: new Concepts in Classification and Treatment. *Am J Clin Dermatol.* 2021;22(4):457–465. doi:10.1007/s40257-021-00595-7
32. Aletaha D, Neogi T, Silman AJ, et al. Rheumatoid arthritis classification criteria: An American College Of Rheumatology/European league against rheumatism Collaborative initiative. *Arthritis Rheum.* 2010;62(9):2569–2581. doi:10.1002/art.27584
33. Pinero J, Sauch J, Sanz F, Furlong LI. The DisGeNET cytoscape app: exploring and visualizing disease genomics data. *Comput Struct Biotech J.* 2021;19:2960–2967. doi:10.1016/j.csbj.2021.05.015
34. Egeberg A, Hansen PR, Gislason GH, Thyssen JP. Clustering of autoimmune diseases in patients with rosacea. *J Am Acad Dermatol.* 2016;74(4):667–672e661. doi:10.1016/j.jaad.2015.11.004
35. Zhou S, Lu H, Xiong M. Identifying immune cell infiltration and effective diagnostic biomarkers in rheumatoid arthritis by bioinformatics analysis. *Front Immunol.* 2021;12:726747. doi:10.3389/fimmu.2021.726747
36. Ahn CS, Huang WW. Rosacea Pathogenesis. *Dermatol Clin.* 2018;36(2):81–86. doi:10.1016/j.det.2017.11.001
37. Lu X, Yarbrough WG. Negative regulation of RelA phosphorylation: emerging players and their roles in cancer. *Cytokine Growth Factor Rev.* 2015;26(1):7–13. doi:10.1016/j.cytogfr.2014.09.003
38. Boutet MA, Courties G, Nerviani A, et al. Novel insights into macrophage diversity in rheumatoid arthritis synovium. *Autoimmun Rev.* 2021;20(3):102758. doi:10.1016/j.autrev.2021.102758
39. Fukui S, Iwamoto N, Takatani A, et al. M1 and M2 Monocytes in Rheumatoid Arthritis: a Contribution of Imbalance of M1/M2 Monocytes to Osteoclastogenesis. *Front Immunol.* 2017;8:1958. doi:10.3389/fimmu.2017.01958
40. Elemam NM, Hannawi S, Maghazachi AA. Role of Chemokines and Chemokine Receptors in Rheumatoid Arthritis. *Immunotargets Ther.* 2020;9:43–56. doi:10.2147/ITT.S243636
41. Maruotti N, Annese T, Cantatore FP, Ribatti D. Macrophages and angiogenesis in rheumatic diseases. *Vasc Cell.* 2013;5(1):11. doi:10.1186/2045-824X-5-11
42. Antonelli A, Ferrari SM, Giuggioli D, Ferrannini E, Ferri C, Fallahi P. Chemokine (C-X-C motif) ligand (CXCL)10 in autoimmune diseases. *Autoimmun Rev.* 2014;13(3):272–280. doi:10.1016/j.autrev.2013.10.010
43. Kwak HB, Ha H, Kim HN, et al. Reciprocal cross-talk between RANKL and interferon-gamma-inducible protein 10 is responsible for bone-erosive experimental arthritis. *Arthritis Rheum.* 2008;58(5):1332–1342. doi:10.1002/art.23372
44. Moura AKA, Guedes F, Rivitti-Machado MC, Sotto MN. Inate immunity in rosacea. Langerhans cells, plasmacytoid dendritic cells, Toll-like receptors and inducible oxide nitric synthase (iNOS) expression in skin specimens: case-control study. *Arch Dermatol Res.* 2018;310(2):139–146. doi:10.1007/s00403-018-1806-z
45. Yamasaki K, Gallo RL. The molecular pathology of rosacea. *J Dermatol Sci.* 2009;55(2):77–81. doi:10.1016/j.jdermsci.2009.04.007
46. Karnezis T, Farnsworth RH, Harris NC, et al. CCL27/CCL28-CCR10 Chemokine Signaling Mediates Migration of Lymphatic Endothelial Cells. *Cancer Res.* 2019;79(7):1558–1572. doi:10.1158/0008-5472.CAN-18-1858
47. Li Y, Yang L, Wang Y, et al. Exploring metformin as a candidate drug for rosacea through network pharmacology and experimental validation. *Pharmacol Res.* 2021;174:105971. doi:10.1016/j.phrs.2021.105971
48. Xiong N, Fu Y, Hu S, Xia M, Yang J. CCR10 and its ligands in regulation of epithelial immunity and diseases. *Protein Cell.* 2012;3(8):571–580. doi:10.1007/s13238-012-2927-3
49. Homey B, Alenius H, Muller A, et al. CCL27-CCR10 interactions regulate T cell-mediated skin inflammation. *Nat Med.* 2002;8(2):157–165. doi:10.1038/nm0202-157
50. Ilchovska DD, Barrow DM. An Overview of the NF- κ B mechanism of pathophysiology in rheumatoid arthritis, investigation of the NF- κ B ligand RANKL and related nutritional interventions. *Autoimmun Rev.* 2021;20(2):102741. doi:10.1016/j.autrev.2020.102741
51. Moschonis G, Manios Y. Skeletal site-dependent response of bone mineral density and quantitative ultrasound parameters following a 12-month dietary intervention using dairy products fortified with calcium and vitamin D: the Postmenopausal Health Study. *Br J Nutr.* 2006;96(6):1140–1148. doi:10.1017/BJN20061977
52. Wladis EJ, Lau KW, Adam AP. Nuclear factor kappa-b is enriched in eyelid specimens of rosacea: implications for pathogenesis and therapy. *Am J Ophthalmol.* 2019;201:72–81. doi:10.1016/j.ajo.2019.01.018

53. Neumann M, Naumann M. Beyond IkappaBs: alternative regulation of NF-kappaB activity. *FASEB J*. 2007;21(11):2642–2654. doi:10.1096/fj.06-7615rev
54. Firestein GS, McInnes IB. Immunopathogenesis of Rheumatoid Arthritis. *Immunity*. 2017;46(2):183–196. doi:10.1016/j.immuni.2017.02.006
55. Steinhoff M, Buddenkotte J, Aubert J, et al. Clinical, cellular, and molecular aspects in the pathophysiology of rosacea. *J Invest Dermatol Symp Proc*. 2011;15(1):2–11. doi:10.1038/jidsymp.2011.7
56. Korbecki J, Kojder K, Siminska D, et al. CC Chemokines in a Tumor: A review of pro-cancer and anti-cancer properties of the ligands of receptors CCR1, CCR2, CCR3, and CCR4. *Int J Mol Sci*. 2020;21(21):8412.
57. Zhong W, Wang B, Yu H, et al. Serum CCL27 predicts the response to Bacillus Calmette-Guerin immunotherapy in non-muscle-invasive bladder cancer. *Oncoimmunology*. 2020;9(1):1776060. doi:10.1080/2162402X.2020.1776060
58. Limagne E, Nuttin L, Thibaudin M, et al. MEK inhibition overcomes chemoimmunotherapy resistance by inducing CXCL10 in cancer cells. *Cancer Cell*. 2022;40(2):136–152e112. doi:10.1016/j.ccell.2021.12.009

Journal of Inflammation Research

Dovepress

Publish your work in this journal

The Journal of Inflammation Research is an international, peer-reviewed open-access journal that welcomes laboratory and clinical findings on the molecular basis, cell biology and pharmacology of inflammation including original research, reviews, symposium reports, hypothesis formation and commentaries on: acute/chronic inflammation; mediators of inflammation; cellular processes; molecular mechanisms; pharmacology and novel anti-inflammatory drugs; clinical conditions involving inflammation. The manuscript management system is completely online and includes a very quick and fair peer-review system. Visit <http://www.dovepress.com/testimonials.php> to read real quotes from published authors.

Submit your manuscript here: <https://www.dovepress.com/journal-of-inflammation-research-journal>